Chapter 4

Prescribed Performance-Based Data-Driven Control Using Minimum Operator For Discrete-Time Nonlinear Systems

4.1 Introduction

DDC approaches are gaining significant traction, as they rely solely on the input and output of the plant. In this chapter, we have used a concept called the pseudo partial derivative (PPD) and pseudo gradient (PG) an approaches to capture the dynamic behavior of the controlled plant, moving away from the traditional state-space representation. This framework includes three different dynamic linearization data models [14] CFDL, PFDL, and FFDL. Among the three, FFDL is the most generalized form, and we have used it for our development purposes. Many practical systems are required to meet prescribed performance (PP) [21], ensuring that both dynamic and equilibrium errors are driven to predefined bounds. Building on the work in [21], various prescribed performance control (PPC) strategies have emerged [22]. However, these methods primarily focus on CTS. Unfortunately, discretizing control signals introduces additional complexity in controller design and stability analysis. Sampling errors further degrade system performance, creating a gap between continuous- and discrete-time control schemes. This gap hinders direct application of continuous-time methods to DTS, underscoring the need for dedicated re-

search in this area. While limited research exists on PPC for DTS [23], a recent attempt was made to formulate MFAC using DSMC with features for PPC [24], where the authors developed a data-driven adaptive SMC strategy based on the FFDL technique. Recently minimum operator based DSMC [2] are developed, however, no prior attempt has been made to integrate the minimum operator-based DSMC approach with FFDL and PPC simultaneously, and the potential for performance improvement through this combination remains unexplored. This paper proposes two FFDL-minimum operator-based DSMC schemes designed for nonlinear PPC.

This chapter introduces several novel contributions for nonlinear discrete-time systems (DTS) with perturbations:

- A controller design framework that integrates the FFDL approach with minima based DSMC.
- The proposed controllers leverage benefit of PPC methods, which is essential for many practical systems.
- We propose an ε-regularized logarithmic PPC that enforces asymmetric, adjustable funnels with a closed-form inverse, enabling direct next-step error set-pointing within an RL1/RL2 FFDL–DSMC framework while preserving numerical robustness and bounded control effort.
- The proposed data-driven control laws ensure finite-time boundedness of the switching function and reduced QSMD, offering improved robust control compared to previous approaches.
- Numerical simulations demonstrate that the PPC-FFDL-minima based DSMC algorithm significantly outperforms other methods in terms of tracking error reduction and disturbance rejection.

4.2 FFDL Data Model

A SISO discrete-time nonlinear system can be represented as:

$$y_{k+1} = f\left(y_k, y_{k-1}, \ldots, y_{k-n_y}, u_k, u_{k-1}, \ldots, u_{k-n_u}\right) + \delta_k \tag{4.1}$$

$y_k \in R$ and $u_k \in R$ denote the output and input of the dynamics, respectively; $n_y > 0$, $n_u > 0$, where $n_y, n_u \in \mathbb{Z}^+$, and $\mathbb{Z}^+$ denotes the set of positive integers. and we have considered $n_y = n_u = 1, \delta_k$ denotes the constrained perturbations such that $\|\delta_k\| \leq \mathcal{D}$, where $\mathcal{D} > 0$.

Assumption 1: The system described by (4.1) exhibits both controllability and observability. In particular, if the target signal y'_{k+1} remains bounded, it follows that the control input u_k will also be constrained, allowing y_{k+1} to accurately track the desired signal y'_{k+1}.

Assumption 2: The DTS (4.1) satisfies a generalized Lipschitz condition, which is expressed as $|\Delta y_{k+1}| \leq b||\xi_k||$ for any k where $\xi_k^T = [\Delta y_k, \Delta u_k]$, with $b > 0$. Here, $\Delta y_k = y_k - y_{k-1}$ and $\Delta u_k = u_k - u_{k-1}$.

Remark 1. From a practical standpoint, Assumption 1 serves as a fundamental prerequisite for ensuring the system's controllability. Assumption 2 implies that a finite variation in the control input does not result in an infinite variation in the system output. Assumptions 1–2 are also discussed in [54], and readers may refer to [54] for further details.

Lemma 1: Examine the nonlinear system (4.1). If $f(\cdot)$ satisfies Assumptions 1 and 2, then there exists PG ϕ_k such that system (4.1) can be expressed as:

$$y_{k+1} = y_k + \phi_{1,k}\Delta y_k + \phi_{2,k}\Delta u_k = y_k + \xi_k^T \phi_k + \delta_k \tag{4.2}$$

where $\phi_k = [\phi_{1,k}, \phi_{2,k}]^T$ is constrained $\forall\ k\ >\ 0$.

4.2.1 Pseudo Partial Derivative Assessment

Based on the approach in [14], an estimate of the unknown vector ϕ_k, denoted by $\hat{\phi}_k$, can be obtained by minimizing the following cost function: $J(\phi_k) = \|\Delta y_k - \zeta_{k-1}^T \phi_k\|^2 + \sigma\|\phi_k - \hat{\phi}_{k-1}\|^2$, where σ is a positive regularization parameter. To find the optimal $\hat{\phi}_k$, we set the derivative of J with respect to ϕ_k to zero, leading to the condition: $\sigma(\phi_k - \hat{\phi}_{k-1}) - \zeta_{k-1}^T(\Delta y_k - \zeta_{k-1}^T \phi_k) = 0$. From this condition, the recursive estimation algorithm is derived as:

$$\hat{\phi}_k = \hat{\phi}_{k-1} + \frac{\kappa\zeta_{k-1}(\Delta y_k - \zeta_{k-1}^T \hat{\phi}_{k-1})}{\sigma + \|\zeta_{k-1}\|^2}, \tag{4.3}$$

where $\kappa \in (0, 2)$ is a gain factor, and $\sigma > 0$ ensures stability.

Remark 1: The updating law (4.3) is designed based solely on the controlled system's input and output measurement data. The stability of this method are analyzed in

detail in [23].

Remark 2: The disturbance estimate $\hat{\delta}k$ of δ_k in (4.2) is obtained via perturbation estimation as $\hat{\delta}k = \delta_{k-1} = y_k - y_{k-1} - \xi_{k-1}^T \phi_{k-1}$. Now (4.2) can be written as:

$$y_{k+1} = y_k + \xi_k^T \hat{\phi}k + \hat{\delta}k - \tilde{\delta}k \tag{4.4}$$

where $\tilde{\delta}k = \delta_{k-1} - \delta_k$, and $\hat{\phi}k$ is estimate of PG.

4.3 Prescribed Performance Function

A discrete-time prescribed performance function (PPF) is adopted to specify a time-varying funnel within which the tracking error must evolve. The sequence $\{\rho_k\}$ is generated as a first-order filter:

$$\rho_{k+1} = (1-\nu)\rho_k + \nu\rho_s, \qquad \rho_0 > \rho_s > 0,\ \nu \in (0,1), \tag{4.5}$$

so that $\lim_{k\to\infty} \rho_k = \rho_s$. The tracking error (TE) $e_k := y_{d,k} - y_k$ is required to satisfy the asymmetric performance bounds

$$-a_k\rho_k \ < \ e_k \ < \ b_k\rho_k, \tag{4.6}$$

where the configurable frontier functions a_k and b_k tighten to one according to

$$a_{k+1} = (1-\nu)a_k + \nu, \quad a_0 \geq 1, \quad b_{k+1} = (1-\nu)b_k + \nu, \quad b_0 \geq 1. \tag{4.7}$$

To enforce (4.6) via a transformed tracking error (TTE), a monotone, bijective error–to–auxiliary map (error transfer function, ETF) is employed. Define the normalized error $\xi_k := e_k/\rho_k \in (-a_k, b_k)$. A *logarithmic barrier* ETF is proposed as:

$$\tau_k \ = \ \frac{1}{2}\ln\!\left(\frac{\xi_k + a_k + \varepsilon}{b_k - \xi_k + \varepsilon}\right), \qquad \varepsilon > 0, \tag{4.8}$$

which, for a small $\varepsilon > 0$ maps the open interval $(-a_k, b_k)$ *bijectively and monotonically* onto $\mathbb{R}$. The inverse map is available in closed form,

$$\xi_k \ = \ \frac{(b_k+\varepsilon)\,e^{2\tau_k} - (a_k+\varepsilon)}{1+e^{2\tau_k}}, \qquad e_k \ = \ \rho_k\,\xi_k, \tag{4.9}$$

From (4.8) it follows that $\tau_k \to +\infty$ as $e_k \uparrow b_k\rho_k$ and $\tau_k \to -\infty$ as $e_k \downarrow -a_k\rho_k$, i.e., a barrier Lyapunov property is realized.

Remark 3. Compared with the tangent-based ETF and logarithmic function based ETF [24], the proposed logarithmic barrier ETF naturally enforces *asymmetric* bounds, respects the true limits $(-a_k, b_k)$, and realizes a strict barrier ($\tau_k \to \pm\infty$ at the bounds) with a closed-form inverse, while offering better numerical conditioning (low gain near $\xi_k \approx 0$, higher near the limits). Hence, the ε-regularized logarithmic barrier is preferable for PPC with asymmetric bounds; the tangent map may dilute the tighter side ($a_k \neq b_k$) and can overflow near its asymptotes.

4.4 Minimum Operator-Based PPC-FFDL-DSMC Design

This section outlines the controller design process of the minimum operator-based PPC-FFDL-DSMC scheme. Initially the controller is designed based on RL1 and RL2 and later the stability of the proposed controller is also demonstrated.

4.4.1 DESIGN OF CONTROLLER USING PPC–FFDL–RL1 SCHEME

Define the TE as

$$e_k \;=\; y'_k - y_k. \tag{4.10}$$

Using the FFDL model, the one-step-ahead error is written as

$$\begin{aligned} e_{k+1} &= y'_{k+1} - y_k - \phi_{1,k}\Delta y_k - \phi_{2,k}\Delta u_k - \hat{\delta}_k + \tilde{\delta}_k \\ &= \psi_k - \phi_{2,k}\Delta u_k, \end{aligned} \tag{4.11}$$

where $\Delta y_k := y_k - y_{k-1}$, $\Delta u_k := u_k - u_{k-1}$, and $\psi_k := y'_{k+1} - y_k - \phi_{1,k}\Delta y_k - \hat{\delta}_k$. The small residual $\tilde{\delta}_k$ is neglected.

The sliding function is defined as

$$\aleph_k \;=\; c\,\tau_k, \tag{4.12}$$

with $c \in \mathbb{R}$; for the SISO case, $c = 1$ is adopted (it may be tuned via level sets).

A boundary-layer version of RL1 (2.4) is imposed using (4.11):

$$\aleph_{k+1} = \tau_{k+1}, \qquad \tau_{k+1} \;=\; \aleph_k - \operatorname{sign}(\aleph_k)\min\{|\aleph_k|, \varsigma\},$$

where $\varsigma > 0$ denotes the boundary-layer width. Using (4.11) and the inverse ETF (4.9) at k+1, the target normalized error becomes

$$\xi_{k+1} = \frac{(b_{k+1} + \varepsilon)\, e^{2\chi_k} - (a_{k+1} + \varepsilon)}{1 + e^{2\chi_k}}, \tag{4.13}$$

The commanded control increment that enforces $e_{k+1} = \rho_{k+1}\xi_{k+1}$ is therefore

$$\Delta u_k^{\text{cmd}} \;=\; \frac{\psi_k - \rho_{k+1}\,\xi_{k+1}}{\phi_{2,k}}.$$

An adaptive/robust realization is employed by replacing $\phi_{2,k}$ with its estimate $\hat{\phi}_{2,k}$:

$$u_{1k}^r = \frac{\iota\,\hat{\phi}_{2,k}}{\gamma + \hat{\phi}_{2,k}^2}\Big(\psi_k - \rho_{k+1}\,\Xi_1(k)\Big), \tag{4.14}$$

where $\gamma > 0,\ \iota \in (0, 1]$,

$$\begin{aligned} \psi_k &:= y'_{k+1} - y_k - \phi_{1,k}\Delta y_k - \hat{\delta}_k, \\ \Xi_1(k) &:= \frac{(b_{k+1} + \varepsilon)\, e^{2\chi_1(k)} - (a_{k+1} + \varepsilon)}{1 + e^{2\chi_1(k)}}, \\ \chi_1(k) &:= \aleph_k - \text{sign}(\aleph_k)\min\{|\aleph_k|, \varsigma\}. \end{aligned} \tag{4.15}$$

The control input is updated as

$$u_{1k} \;=\; u_{1,k-1} + u_{1k}^r. \tag{4.16}$$

4.4.2 DESIGN OF CONTROLLER USING PPC-FFDL-RL2 SCHEME

Consider the same TE (4.10) and sliding function (4.12). The PPC–FFDL–RL2-based control law is obtained as follows. Impose the RL2 manifold with a boundary layer:

$$\begin{aligned} \aleph_{k+1} &= \tau_{k+1}, \\ \tau_{k+1} &= \aleph_k \;-\; \varsigma\,\text{sign}(\aleph_k)\,\min\!\left(\frac{|\aleph_k|}{\varsigma},\, |\aleph_k|^{\beta}\right), \end{aligned} \tag{4.17}$$

Here, $\varsigma > 0,\ \beta \in (0, 1)$ together with (4.11) and the inverse ETF (4.9) at k+1, the target normalized error becomes

$$\begin{aligned} \xi_{k+1} &= \frac{(b_{k+1} + \varepsilon)\, e^{2\chi_k} - (a_{k+1} + \varepsilon)}{1 + e^{2\chi_k}}, \\ \chi_k &= \aleph_k - \varsigma\ \text{sign}(\aleph_k)\ \min\!\left(\frac{|\aleph_k|}{\varsigma},\, |\aleph_k|^{\beta}\right). \end{aligned}$$

so that $e_{k+1} = \rho_{k+1}\xi_{k+1}$ and the commanded increment becomes

$$\Delta u_k^{\mathrm{cmd}} = \frac{\psi_k - \rho_{k+1}\,\xi_{k+1}}{\phi_{2,k}}.$$

An adaptive/robust realization is

$$u_{2k}^r = \frac{\iota\,\hat{\phi}_{2,k}}{\gamma + \hat{\phi}_{2,k}^2}\left(\psi_k - \rho_{k+1}\,\Xi_2(k)\right) \tag{4.18}$$

with $\gamma > 0$ and $\iota \in (0, 1]$. The control input is updated as

$$u_{2k} \;=\; u_{2,k-1} + u_{2k}^r. \tag{4.19}$$

where,

$$\begin{aligned} \Xi_2(k) &= \frac{(b_{k+1} + \varepsilon)\,e^{2\chi_k} - (a_{k+1} + \varepsilon)}{1 + e^{2\chi_k}}, \\ \chi_k &= \aleph_k - \varsigma\ \mathrm{sign}(\aleph_k)\ \min\!\left(\frac{|\aleph_k|}{\varsigma},\ |\aleph_k|^{\beta}\right). \end{aligned} \tag{4.20}$$

Remark 6. The proposed sliding function (4.12) features a simple structure that avoids the need for additional user-selected gains in designing the sliding plane, unlike the approach in [24]. Furthermore, the control methodology (4.16)–(4.19) exploits the reaching phase to reduce control effort compared with the equivalent control strategy in [24].

4.4.3 STABILITY ANALYSIS

Theorem 1. If Assumptions 1–2 hold for (4.1), the initial condition satisfies $-a_0\rho_0 < e_0 < b_0\rho_0$, the estimator update $\Delta\hat{\phi}_k$ and ETF τ_k are generated by (4.3) and (4.8), and the controller (4.14), (4.16) is applied with an RL1 step size ς chosen such that $\varsigma > \omega_m \geq \sup_k |\tilde{\delta}_k|$, then the tracking error (TE) remains in the prescribed performance funnel (4.6) for all k, the sliding signal $\aleph_k$ is ultimately bounded, and the control input u_{1k} is bounded (trivially so if actuator projection $u_{1k} \in [u_{\min}, u_{\max}]$ is used).

Proof.

Step 1 (Finite-time boundedness of the switching signal). From (2.4) and (4.12) we obtain

$$\tau_{k+1} = \aleph_{k+1} = \aleph_k - \mathrm{sign}(\aleph_k)\min\{|\aleph_k|, \varsigma\} + \tilde{\delta}_k. \tag{4.21}$$

Let $V(k) := |\aleph_k|$ and define $b_k := \aleph_k - \mathrm{sign}(\aleph_k)\min\{|\aleph_k|, \varsigma\}$, so $|b_k| = |\aleph_k| - \min\{|\aleph_k|, \varsigma\}$. Using the triangle inequality,

$$\Delta V(k) = |b_k + \tilde{\delta}_k| - |\aleph_k| \leq -\min\{|\aleph_k|, \varsigma\} + |\tilde{\delta}_k|.$$

Hence, if $|\aleph_k| \geq \varsigma$ then $\Delta V(k) \leq -(\varsigma - |\tilde{\delta}_k|) \leq -(\varsigma - \omega_m) < 0$; if $|\aleph_k| \leq \varsigma$ then $\Delta V(k) \leq -(|\aleph_k| - \omega_m)$, so one more step renders $|\aleph_{k+1}| \leq \omega_m$. Therefore,

$$|\aleph_k| \leq \omega_m \quad \text{for all } k \geq \left\lceil \frac{|\aleph_0| - \omega_m}{\varsigma - \omega_m} \right\rceil.$$

Step 2 (Funnel invariance: ideal case). Substituting (4.14), (4.16) into (4.11) gives

$$e_{k+1} = \psi_k - \phi_{2,k} \frac{\iota\, \hat{\phi}_{2,k}}{\gamma + \hat{\phi}_{2,k}^2} \big(\psi_k - \rho_{k+1}\Xi_1(k)\big). \tag{4.22}$$

For the certainty–equivalence case $\hat{\phi}_{2,k} = \phi_{2,k}$, set $\kappa_k := \frac{\iota\, \phi_{2,k}^2}{\gamma + \phi_{2,k}^2} \in (0,1)$ to obtain

$$e_{k+1} = (1 - \kappa_k)\, \psi_k + \kappa_k\, \rho_{k+1}\Xi_1(k).$$

With the commanded increment as in (4.14), $\psi_k \mapsto \rho_{k+1}\Xi_1(k)$ and $e_{k+1} = \rho_{k+1}\Xi_1(k)$. The ε–log–barrier ETF $\tau_k = \frac{1}{2}\ln\!\big(\frac{\xi_k + a_k + \varepsilon}{b_k - \xi_k + \varepsilon}\big)$ is strictly increasing and has a closed-form inverse mapping a *finite* interval in τ onto $\xi \in (-a_k, b_k)$. The RL1 update $\tau_{k+1} = \chi_k := \aleph_k - \operatorname{sign}(\aleph_k)\min\{|\aleph_k|, \varsigma\}$ is a *contraction* in τ, so for any ς small enough that χ_k remains within the inverse's domain, we have

$$\xi_{k+1} = \frac{(b_{k+1} + \varepsilon)e^{2\chi_k} - (a_{k+1} + \varepsilon)}{1 + e^{2\chi_k}} \in (-a_{k+1},\, b_{k+1}), \tag{4.23}$$

and hence $-a_{k+1}\rho_{k+1} < e_{k+1} < b_{k+1}\rho_{k+1}$. Since $-a_0\rho_0 < e_0 < b_0\rho_0$ by hypothesis, induction yields

$$-a_k\rho_k < e_k < b_k\rho_k, \qquad \forall k \in \mathbb{N}. \tag{4.24}$$

Step 3 (Funnel invariance: non-ideal estimate). Define the possibly mismatched contraction gain

$$\tilde{\kappa}_k := \frac{\iota\, \phi_{2,k}\, \hat{\phi}_{2,k}}{\gamma + \hat{\phi}_{2,k}^2},$$

so that

$$e_{k+1} - \rho_{k+1}\Xi_1(k) = (1 - \tilde{\kappa}_k)\big(\psi_k - \rho_{k+1}\Xi_1(k)\big). \tag{4.25}$$

Assume a standard projection $\hat{\phi}_{2,k} \in [\phi_{2,\min}, \phi_{2,\max}]$ with $\phi_{2,\min} > 0$. Using $0 \leq \frac{x}{\gamma + x^2} \leq \frac{1}{2\sqrt{\gamma}}$ for $x \geq 0$, we get $0 < \underline{\kappa} \leq \tilde{\kappa}_k \leq \bar{\kappa} < 1$ by suitable $\gamma > 0$ (and/or $\iota \in (0,1]$). Thus (4.25) is a contraction toward $\rho_{k+1}\Xi_1(k)$, and the same induction as in Step 2 yields (4.24).

Step 4 (Boundedness of the input). From (4.14),

$$|\Delta u_k| = \left| \frac{\iota\, \hat{\phi}_{2,k}}{\gamma + \hat{\phi}_{2,k}^2} \right| \big|\psi_k - \rho_{k+1}\Xi_1(k)\big| \leq \frac{\iota}{2\sqrt{\gamma}} \Big(|\psi_k| + \rho_{k+1}|\Xi_1(k)| \Big),$$

and the right–hand side is bounded because of (4.24) and bounded regressors/disturbance (Assumptions 1–2). With actuator projection $u_{1k} \in [u_{\min}, u_{\max}]$, the input is trivially bounded; without projection, boundedness follows under the usual adaptive conditions, ensuring summability of the residual. □

Remark 7. Choose $\varsigma > \omega_m$ to secure the finite-time bound in Step 1; pick $\varepsilon > 0$ to avoid singularities at the funnel edges and ensure a well-posed inverse; select $\gamma > 0$ (and $\iota \in (0, 1]$) so that the contraction gains satisfy $0 < \kappa_k, \tilde{\kappa}_k < 1$ uniformly by the bound $\sup_{x \geq 0} \frac{x}{\gamma + x^2} = \frac{1}{2\sqrt{\gamma}}$.

Theorem 2. If Assumptions 1–2 hold for (4.1), the initial condition satisfies $-a_0\rho_0 < e_0 < b_0\rho_0$, the estimator update $\Delta\hat{\phi}_k$ and the ETF τ_k are generated by (4.3) and (4.8), and the RL2 controller (4.18), (4.19) is applied with $0 < \beta < 1$ and $\varsigma > \omega_m \geq \sup_k |\tilde{\delta}_k|$, then the tracking error (TE) satisfies the prescribed performance bounds (4.6) for all k, while the sliding signal $\aleph_k$ and the input u_{2k} remain bounded.

Proof.

Step 1 (Ultimate boundedness of the switching signal). The RL2 manifold with boundary layer reads (cf. (4.17))

$$\tau_{k+1} = \aleph_{k+1} = \aleph_k - \varsigma \operatorname{sign}(\aleph_k) \min\Big(\tfrac{|\aleph_k|}{\varsigma},\, |\aleph_k|^{\beta}\Big) + \tilde{\delta}_k. \tag{4.26}$$

Let $V(k) := |\aleph_k|$. Using the triangle inequality and $|x - \operatorname{sign}(x)\min(|x|/\varsigma, |x|^{\beta})| = |x| - \min(|x|,\, \varsigma|x|^{\beta})$, we get

$$\begin{aligned} \Delta V(k) &= |\aleph_{k+1}| - |\aleph_k| \\ &\leq -\min\big(|\aleph_k|,\, \varsigma|\aleph_k|^{\beta}\big) + |\tilde{\delta}_k| \\ &\leq -\min\big(|\aleph_k|,\, \varsigma|\aleph_k|^{\beta}\big) + \omega_m. \end{aligned}$$

Hence: (i) if $|\aleph_k| \geq r_* := \big(\omega_m/\varsigma\big)^{1/\beta}$, then $\Delta V(k) \leq -\varsigma|\aleph_k|^{\beta} + \omega_m \leq 0$ with strict decrease for $|\aleph_k| > r_*$; and (ii) if $|\aleph_k| \leq \varsigma$, then $\Delta V(k) \leq -|\aleph_k| + \omega_m \leq -(\varsigma - \omega_m)$ whenever $|\aleph_k| \geq \varsigma$. Therefore, $|\aleph_k|$ reaches in finite time the compact set $\mathcal{B}_\omega := \{\, |\aleph| \leq \bar{\omega} \,\}$ with $\bar{\omega} := \max\big\{\varsigma,\, (\omega_m/\varsigma)^{1/\beta}\big\}$, and stays there. In particular, $\aleph_k$ is ultimately bounded.

Step 2 (Funnel invariance via the –log barrier). Let $\xi_k := e_k/\rho_k$ and use the regularized log–barrier ETF $\tau_k = \frac{1}{2}\ln\big(\frac{\xi_k + a_k + \varepsilon}{b_k - \xi_k + \varepsilon}\big)$, $\varepsilon > 0$, with inverse

$$\mathcal{T}_{\log}^{-1}(\tau; a, b, \varepsilon) = \frac{(b + \varepsilon)e^{2\tau} - (a + \varepsilon)}{1 + e^{2\tau}}.$$

With the RL2 update (4.26) define

$$\chi_k := \aleph_k - \varsigma\,\mathrm{sign}(\aleph_k)\,\min\Big(\tfrac{|\aleph_k|}{\varsigma},\,|\aleph_k|^{\beta}\Big),$$

so that $\tau_{k+1} = \chi_k + \tilde{\delta}_k$. Because $\aleph_k$ is ultimately bounded (Step 1) and $\tilde{\delta}_k$ is bounded, τ_{k+1} remains in a compact interval on which the inverse ETF is well defined. Therefore the *target* normalized error at $k{+}1$,

$$\xi_{k+1} = \mathcal{T}_{\log}^{-1}\big(\chi_k;\, a_{k+1}, b_{k+1}, \varepsilon\big) = \frac{(b_{k+1}+\varepsilon)e^{2\chi_k} - (a_{k+1}+\varepsilon)}{1+e^{2\chi_k}},$$

satisfies $\xi_{k+1} \in (-a_{k+1}, b_{k+1})$, hence $-a_{k+1}\rho_{k+1} < \rho_{k+1}\xi_{k+1} < b_{k+1}\rho_{k+1}$.

Step 3 (Closed-loop one–step error and invariance). From (4.11) and the RL2 realization (4.18), (4.19),

$$\begin{aligned} e_{k+1} &= \psi_k - \phi_{2,k}\,\frac{\iota\,\hat{\phi}_{2,k}}{\gamma+\hat{\phi}_{2,k}^2}\Big(\psi_k - \rho_{k+1}\,\Xi_2(k)\Big), \\ \Xi_2(k) &:= \mathcal{T}_{\log}^{-1}\big(\chi_k;\, a_{k+1},\, b_{k+1},\, \varepsilon\big). \end{aligned} \tag{4.27}$$

(i) Ideal estimate) If $\hat{\phi}_{2,k} = \phi_{2,k}$, set $\kappa_k := \frac{\iota\,\phi_{2,k}^2}{\gamma+\phi_{2,k}^2} \in (0,1)$ to obtain $e_{k+1} = (1-\kappa_k)\psi_k + \kappa_k\,\rho_{k+1}\Xi_2(k)$. Choosing the commanded increment as in (4.18) makes $\psi_k \mapsto \rho_{k+1}\Xi_2(k)$, whence $e_{k+1} = \rho_{k+1}\Xi_2(k) \in (-a_{k+1}\rho_{k+1},\, b_{k+1}\rho_{k+1})$. *(ii) Non-ideal estimate)* With the contraction gain $\tilde{\kappa}_k := \frac{\iota\,\phi_{2,k}\hat{\phi}_{2,k}}{\gamma+\hat{\phi}_{2,k}^2}$ and a standard projection $\hat{\phi}_{2,k} \in [\phi_{2,\min}, \phi_{2,\max}]$, one gets

$$|e_{k+1} - \rho_{k+1}\Xi_2(k)| \le (1-\underline{\kappa})\,|\psi_k - \rho_{k+1}\Xi_2(k)|$$

for some $0 < \underline{\kappa} < 1$ (choose $\gamma > 0$, $\iota \in (0,1]$ accordingly). Since $\Xi_2(k) \in (-a_{k+1}, b_{k+1})$ and ψ_k is bounded under Assumptions 1–2, the same induction as in Theorem 1 yields

$$-a_k\rho_k < e_k < b_k\rho_k, \qquad \forall k \in \mathbb{N}. \tag{4.28}$$

Step 4 (Boundedness of the input). From (4.18),

$$|\Delta u_{2k}| = \Big|\tfrac{\iota\,\hat{\phi}_{2,k}}{\gamma+\hat{\phi}_{2,k}^2}\Big|\,|\psi_k - \rho_{k+1}\Xi_2(k)| \le \tfrac{\iota}{2\sqrt{\gamma}}\Big(|\psi_k| + \rho_{k+1}|\Xi_2(k)|\Big),$$

which is uniformly bounded due to (4.28) and Assumptions 1–2. Thus u_{2k} is bounded (trivially so if projected onto $[u_{\min}, u_{\max}]$).

4.5 RESULTS AND DISCUSSION

To validate the performance of the PPC-FFDL-RL1 and PPC-FFDL-RL2 control schemes, this section presents numerical simulations using robotic manipulator. Additionally, to highlight the characteristics of the proposed method, comparisons are made with [24] for both proposed algorithms.

Table 4.1: MSE Comparison

Control Scheme	**[24]**	**FFDL-RL1**	**FFDL-RL2**
MSE 250	0.00492	0.00331	0.00335

4.5.1 NUMERICAL SIMULATION

Consider a robotic manipulator, whose dynamics are described as follows [24]:

$$J\ddot{\theta} + f\dot{\theta} + \left(\frac{1}{2}m + M\right) gl\sin(\theta) = u + d, \tag{4.29}$$

where, θ, $\dot{\theta}$, and $\ddot{\theta}$ represent the angular displacement, angular velocity, and angular acceleration of the manipulator, respectively. u is the driving torque. g is the gravitational acceleration. m, M, l, and f are the link mass, tip load, length, and damping coefficient of the manipulator, respectively. J is the joint moment of inertia, defined as $J = Ml^2 + \frac{1}{3}ml^2$. d represents an external disturbance. Define the state variables as $z_1 = \theta$ and $z_2 = \dot{\theta}$. Using these definitions, the system equation can be rewritten in state-space form:

$$\dot{z}_1 = z_2,\ \dot{z}_2 = \frac{1}{J}\left(-f\dot{z}_2 - \left(\frac{1}{2}m + M\right) gl\sin(z_1) + u + d\right),$$
$$y = z_2.$$

To implement the system in a discrete-time framework, the equations are discretized, yielding:

$$\begin{aligned} y(t+1) &= f(y(t), y(t-1), \ldots, y(0); u(t); d(t)) \\ &= \left(1 - \frac{hf}{J}\right) y(t) - \frac{h}{J}\left(\tfrac{1}{2}m + M\right) gl\sin\big(x_1(0) + E^\top Y(t-1)\big) \\ &\quad + \frac{h}{J}u(t) + \frac{h}{J}d(t). \end{aligned}$$

where, h is the sampling period, $z_1(0)$ is the initial value of $z_1(t)$, $E = [1, \ldots, 1]^\top$, $Y(t-1) = [y(0), \ldots, y(t-1)]^\top$. The true parameter values of the system are specified as $m = 1\,\text{kg}, M = 2\,\text{kg}, l = 0.5\,\text{m}, f = 3\,\text{kg}\cdot\text{m}^2/\text{s}, g = 9.8\,\text{m/s}^2$. The angular velocity, $\dot{\theta}$, is considered as the output of the manipulator. For the simulation purpose, the initial values are set as $u_0 = z_0 = y_0 = 0$, and the sampling time is defined as $h = 0.004$ seconds. The parameters for the proposed control are chosen to be the same as those in [24] to ensure the results are comparable. $\kappa = 0.05, \sigma = 0.15, \lambda = 150, \iota = 0.9, \gamma = 0.00001, \tau_s = 0.001., \beta = 1.1, \varsigma = 0.1$ The initial estimate of $\hat{\phi}_k$ is specified as $\hat{\phi}_0 = [1.1, 0.004]^T$. The PP parameters are defined as: $a_0 = 1.3, \quad b_0 = 1.1, \quad \rho_0 = 1.5, \quad \rho_\infty = 0.05, \quad \nu = 0.08.$

To assess the tracking performance of the two proposed approaches mean squared errors (MSE) and maximum control input of these methods are compared with those presented in [24] in Table I. The MSE is computed using the formula $\text{MSE}_n = \frac{1}{n}\sum_{k=1}^{n}(y_{d,k} - y_k)^2$, where n represents the total number of time steps, which is set to 250 in this example. As illustrated in Table I, PPC-FFDL-RL1 and PPC-FFDL-RL2, demonstrate a reduction in MSE by 33.1% and 33.5%, respectively, compared to [24]. This further reinforces the effectiveness of the proposed approach. The simulation results indicate that the proposed method successfully tracks the reference signal, improving steady-state performance while reducing chattering phenomena. By incorporating DSMC, as presented in [2], and FFDL, the steady-state tracking performance is further enhanced. Additionally, with the inclusion of PPC, the method achieves improved settling times and reduced TE. The TE of the PPC-FFDL-RL1 strategy are compared with those in [24] in Figs. 1(a) and 1(b), illustrating both transient and steady-state performance. A non-symmetric performance constraint is plotted, demonstrating that the PPC-FFDL-RL1 keeps the TE within the performance constraint, as outlined in (4.6).

Furthermore, the TEs of the PPC-FFDL-RL2 strategy are compared with those in [24] in Figs. 1(e) and 1(f), showing both transient and steady-state performance. To evaluate the robustness of the proposed solution against measurement noise of varying magnitudes, a further simulation is conducted. In this case, the PP parameters are changed to $a_0 = b_0 = 2$, $\rho_0 = 1.5$, and $\rho_\infty = 0.25$, while keeping other parameters remain same. The measurement noise levels are considered as $n_{1,k} \in (0, 0.1)$, $n_{2,k} \in (0, 0.2)$, and $n_{3,k} \in (0, 0.3)$, respectively. Figs. 1(d) and 1(h) demonstrate that the proposed method PPC-FFDL-RL1 & RL2 effectively tracks the reference signal, even under varying noise

levels. When $\rho_\infty = 0.25$, and the high noise level $n_{3,k} \in (0, 0.3)$ is present, the control output successfully tracks the reference signal, ensuring that the tracking error (TE) remains within the predefined limits. In conclusion, the proposed strategy ensures the PP within a range of noise levels.

Important performance parameter observations

- κ, σ , γ: This parameter facilitates the convergence of the tracking error to zero at steady state, ensuring accurate final performance.
- β and ς : These parameters collectively influence the rate of control input.
- ν : A smaller value of ν reduces the convergence rate of the error boundaries, effectively controlling how quickly the boundary functions $a(k)$ and $b(k)$ adapt over time.
- ρ_0, a_0, b_0: These parameters govern the initial bounds of the prescribed performance function. Together, they define the initial performance envelope for error evolution.

4.6 Conclusion

This work addressed prescribed-performance control (PPC) for nonlinear discrete-time systems with unknown dynamics. We proposed a data-driven adaptive DSMC framework built on FFDL and a minimum-operator sliding manifold, together with a regularized logarithmic-barrier error–transfer function (ETF) that maps the constrained tracking error to an unconstrained variable. Using this transformed error and the minimum operator, two PPC–FFDL–DSMC laws (RL1 and RL2) were derived. Compared with existing approaches, the proposed controllers retain a simple structure while achieving reduced mean squared error (MSE) with lower control effort. Rigorous analysis establishes forward invariance of the error within the prescribed asymmetric funnel and boundedness of all closed-loop signals. Simulation studies on a robotic manipulator corroborate the theoretical results.

Future research directions include: (i) extending the framework to multi-variable and multi-agent systems, (ii) investigating identifiability and consistency issues associated with performance funnels, (iii) integrating learning-based components (e.g., safe reinforcement

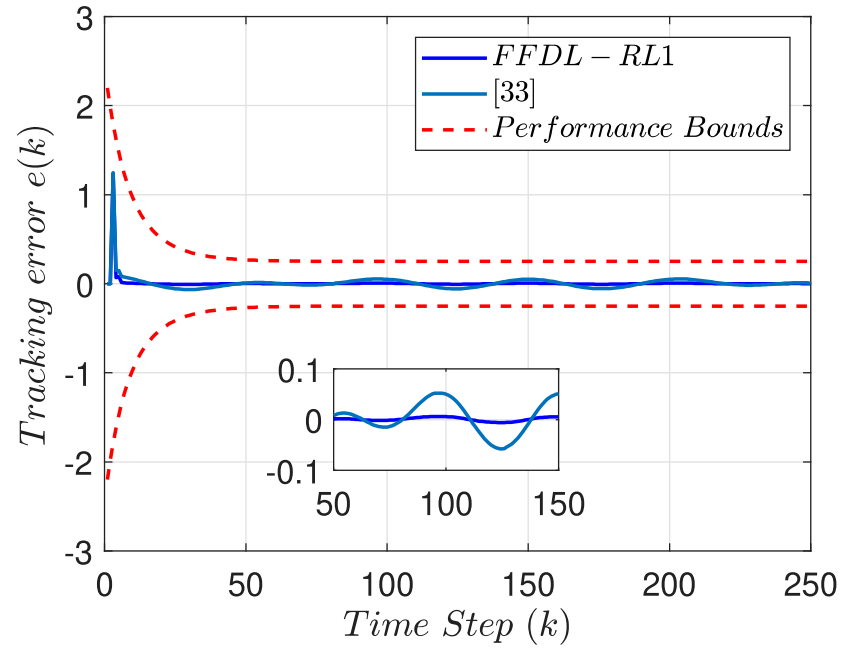

(a) Results of PPC-FFDL-RL1 scheme tracking error

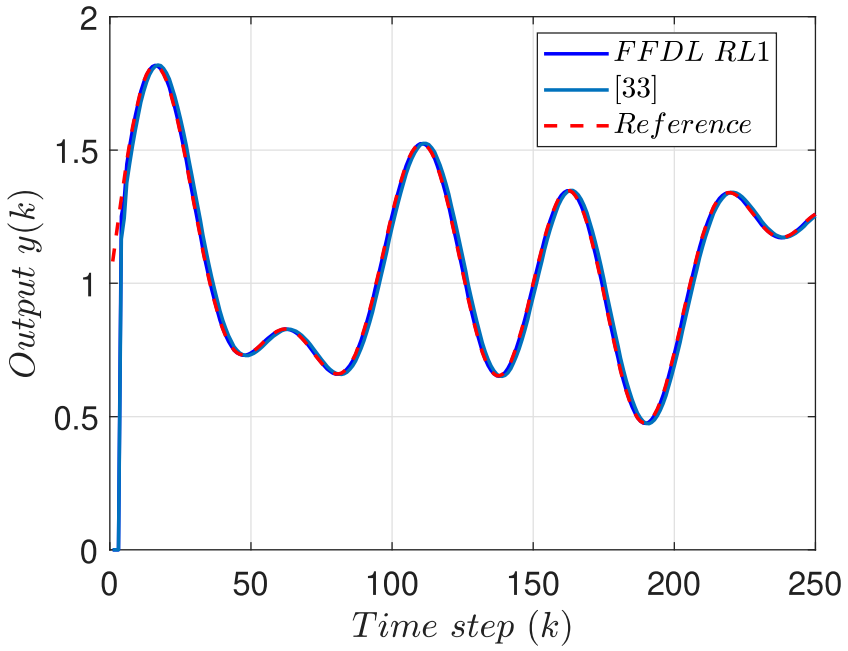

(b) Results of PPC-FFDL-RL1 scheme tracking performance

Figure 4.1: Overview of the PPC-FFDL-RL1 scheme results

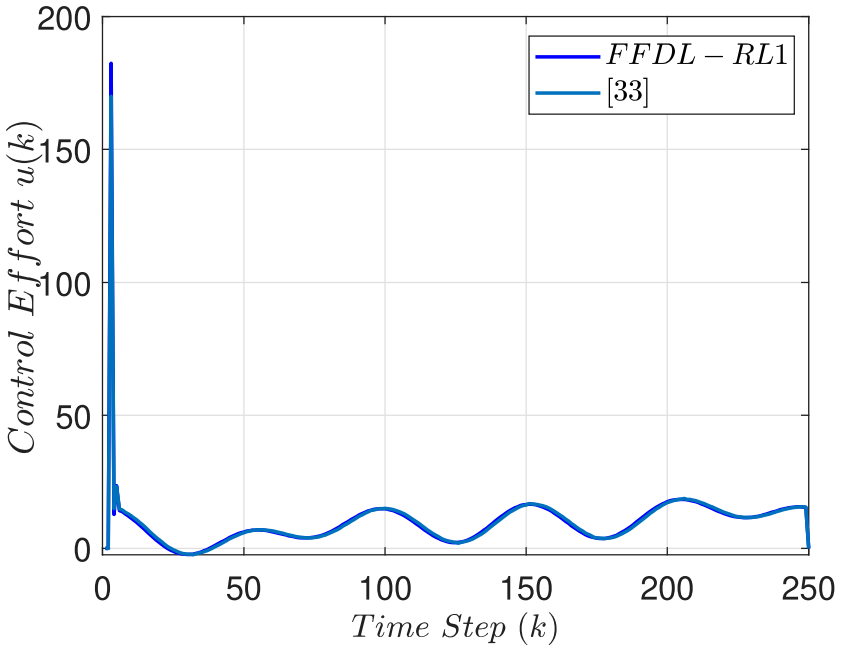

(a) Results of PPC-FFDL-RL1 control input

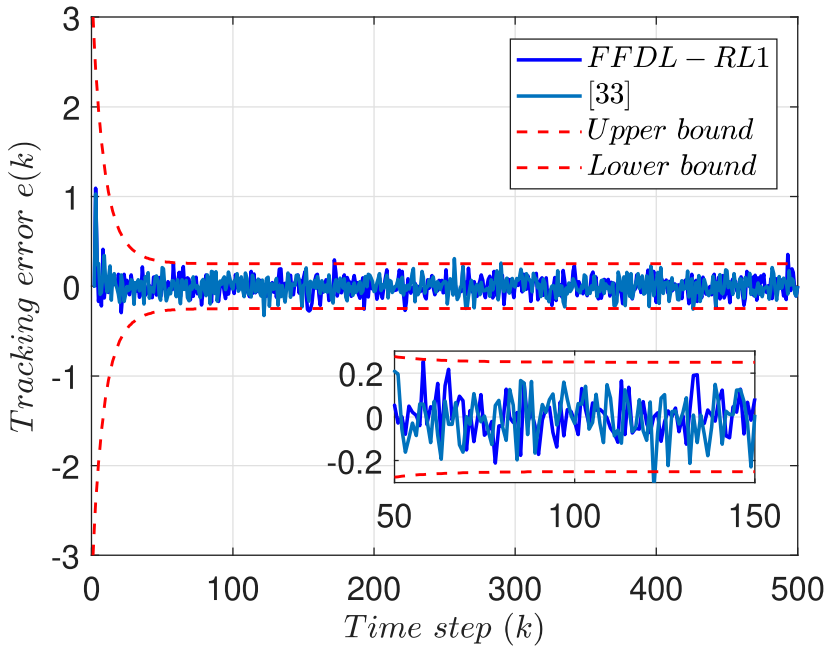

(b) Results of PPC-FFDL-RL1 scheme TE in varying noise level

Figure 4.2: Overview of the PPC-FFDL-RL1 scheme results

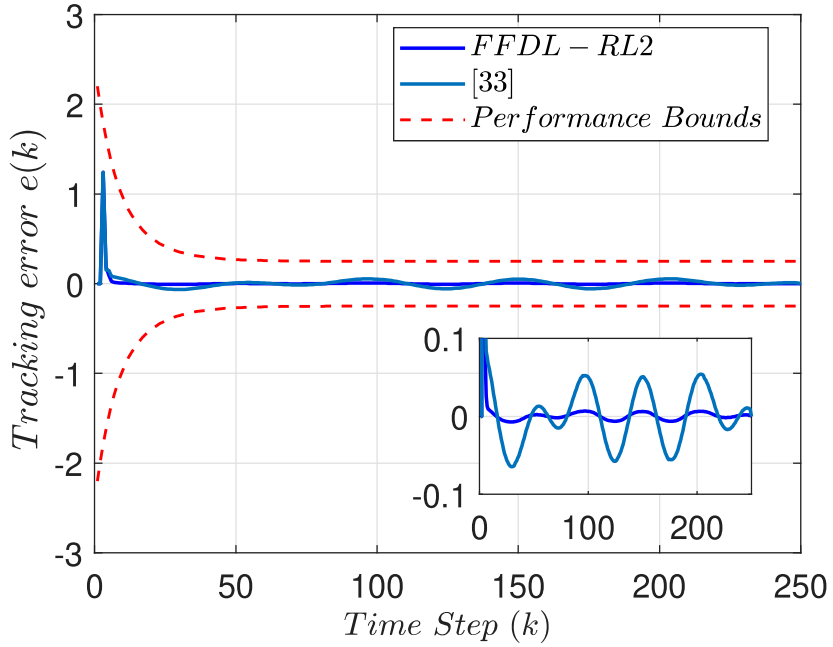

(a) Results of PPC-FFDL-RL2 scheme tracking error

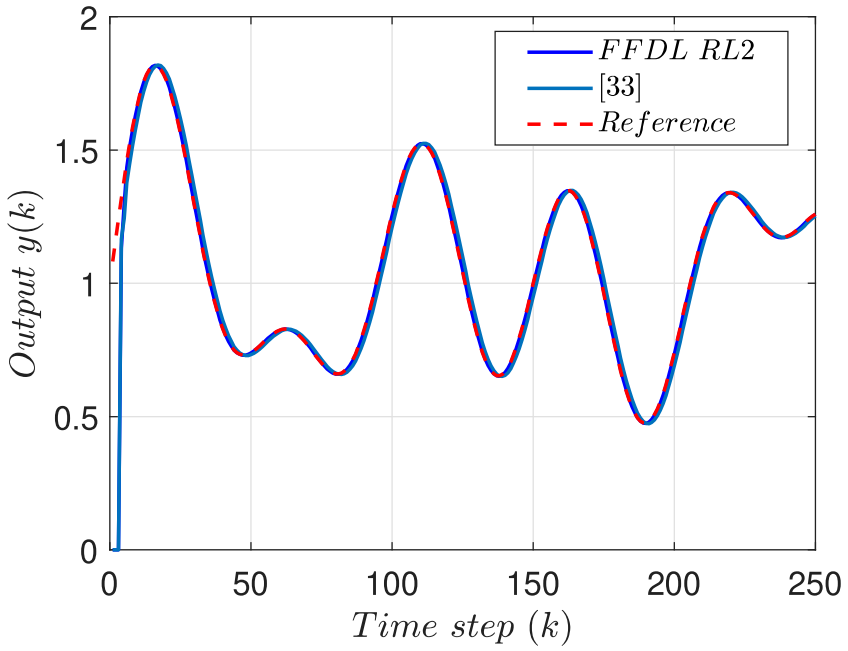

(b) Results of PPC-FFDL-RL2 scheme tracking performance

Figure 4.3: Overview of the PPC-FFDL-RL2 scheme results

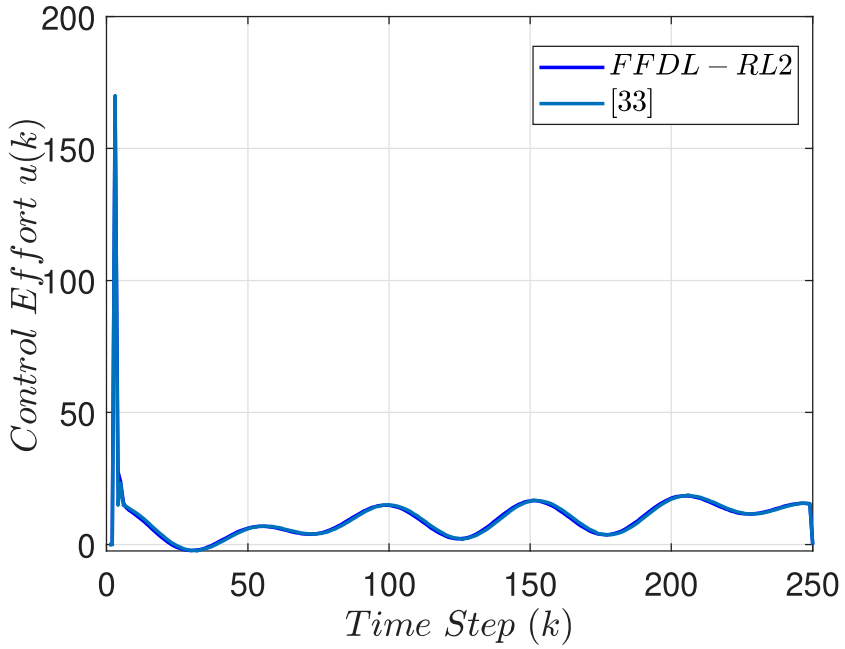

(a) Results of PPC-FFDL-RL2 control input

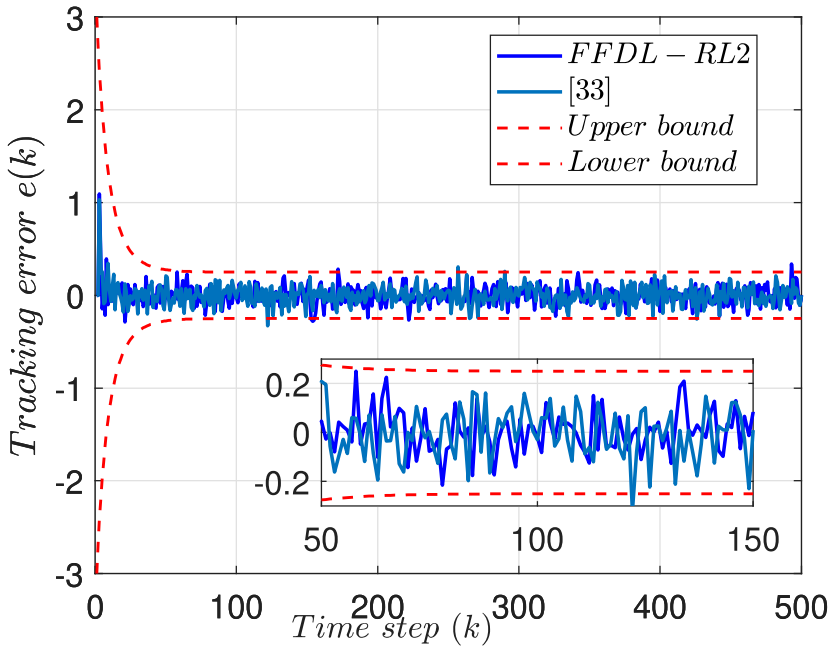

(b) Results of PPC-FFDL-RL2 scheme TE in varying noise level

Figure 4.4: Overview of the PPC-FFDL-RL2 scheme results

learning or adaptive MPC) to enable online policy improvement under safety constraints and time-varying operating conditions, (iv) extending the framework to weakly excited systems and (v) addressing scenarios with limited excitation or constrained actuation.

Algorithm 1 PPC–FFDL–DSMC (RL1/RL2) Controller

Require: Initial (a_0, b_0, ρ_0), $\hat{\phi}_0 = [\hat{\phi}_{1,0}, \hat{\phi}_{2,0}]^\top$, gains $(\nu, \kappa, \beta, \iota, \gamma, \varepsilon, \varsigma, \beta_{\mathrm{RL2}})$

for $k = 0, 1, 2, \ldots$ **do**

PPF update: $\rho_{k+1} = (1-\nu)\rho_k + \nu\rho_s$, $a_{k+1} = (1-\nu)a_k + \nu$, $b_{k+1} = (1-\nu)b_k + \nu$.

Measure/preview: Acquire y_k and r_{k+1} (use $r_{k+1} \approx r_k$ if ZOH).

Error & ETF: $e_k = r_k - y_k$, $\xi_k = \frac{e_k}{\rho_k}$,

$$\tau_k = \tfrac{1}{2} \ln\left(\frac{\xi_k + a_k + \varepsilon}{b_k - \xi_k + \varepsilon}\right).$$

Sliding update:

if RL1 **then**

$\chi_k = \tau_k - \operatorname{sign}(\tau_k) \min\{|\tau_k|, \varsigma\}$

else if RL2 **then**

$\chi_k = \tau_k - \varsigma \operatorname{sign}(\tau_k) \min\left(\frac{|\tau_k|}{\varsigma},\ |\tau_k|^{\beta_{\mathrm{RL2}}}\right)$

end if

Inverse ETF target:

$$\Xi(k) = \frac{(b_{k+1} + \varepsilon)e^{2\chi_k} - (a_{k+1} + \varepsilon)}{1 + e^{2\chi_k}}, \quad e^\star_{k+1} = \rho_{k+1}\, \Xi(k).$$

FFDL update (normalized):

$\zeta_{k-1} = \begin{bmatrix} \Delta y_{k-1} \\ \Delta u_{k-1} \end{bmatrix} = \begin{bmatrix} y_k - y_{k-1} \\ u_k - u_{k-1} \end{bmatrix}$, $\Delta y_k = y_{k+1} - y_k$ (or its measured/estimated proxy).

$\hat{\phi}_k = \hat{\phi}_{k-1} + \kappa \dfrac{\zeta_{k-1}\big(\Delta y_k - \zeta_{k-1}^\top \hat{\phi}_{k-1}\big)}{\beta + \|\zeta_{k-1}\|^2}$.

Predictor: $\psi_k = r_{k+1} - y_k - \hat{\phi}_{1,k} \Delta y_k$.

Control increment: $u_k^r = \dfrac{\iota\, \hat{\phi}_{2,k}}{\gamma + \hat{\phi}_{2,k}^2} \big(\psi_k - e^\star_{k+1}\big)$.

Integrate/saturate: $u_k = u_{k-1} + u_k^r$; apply actuator limits if needed.

end for